Ratio model for suprathreshold hue-increment detection

Marcel J. Sankeralli and Kathy T. Mullen

McGill Vision Research, Department of Ophthalmology, McGill University, Montreal H3A 1A1, Canada

We use psychophysical techniques to investigate the neural mechanisms subserving suprathreshold chromatic discrimination in human vision. We address two questions: (1) How are the postreceptoral detection mechanism responses combined to form suprathreshold chromatic discriminators? and (2) How do these discriminators contribute to color perception? We use a pedestal paradigm in which the subject is required to distinguish between a pedestal stimulus and the same pedestal added to a chromatic increment (the test). Our stimuli are represented in a cardinal space, in which the axes express the responses of the three postreceptoral detection mechanisms normalized relative to their respective detection thresholds. In the main experiment the test (a hue increment) was fixed in the direction orthogonal to the pedestal in our cardinal space. We found that, for high pedestal contrasts, the test threshold varied proportionally with the pedestal contrast. This result suggests the presence of a hue-increment detector dependent on the ratio of the outputs from the red–green and blue–yellow postreceptoral detection mechanisms. The exception to this was for pedestals and tests fixed along the cardinal axes. In that case detection was enhanced by direct input from the postreceptoral mechanism capable of detecting the test in isolation. Our results also indicate that discrimination in the red–green/luminance and blue–yellow/luminance planes exhibits a behavior similar to discrimination within the isoluminant plane. In the final experiment we observed that thresholds for hue-increment identification (e.g., selecting the bluer of two stimuli) are also governed by a ratio relationship. This finding suggests that our ratio-based mechanisms play an important role in color-difference perception. © 1999 Optical Society of America [S0740-3232(99)01711-1]

OCIS codes: 330.1720, 330.5510, 330.6180.

1. INTRODUCTION

There is substantial evidence that outputs from the three cone types [long- (L), middle- (M), and short-wavelength-sensitive (S)] are recombined to form three postreceptoral mechanisms: a cone-additive luminance mechanism responsible for achromatic detection and two cone-opponent mechanisms, labeled red–green and blue–yellow, mediating the detection of isoluminant stimuli (see Ref. 1 for a review). There is, however, additional evidence demonstrating that higher-order processes with inputs from the postreceptoral detectors play an active role in the chromatic discrimination of suprathreshold stimuli.[2] Two interesting questions thus arise: (1) How are the postreceptoral detection mechanism responses combined to form suprathreshold chromatic discriminators? and (2) How do these discriminators contribute to color perception? We address these questions in the present study.

Krauskopf *et al.*[2] performed an adaptation experiment in which the detection threshold of a 1-Hz sinusoidally flickering test spot was measured following exposure to a fixed adaptive field. They showed that, for each adaptive field, masking of the test stimulus was maximal when the test color-space direction was the same as that of the adaptive field. This finding suggests the existence of suprathreshold chromatic discriminators tuned specifically to each selected adaptive-field color-space direction. In a further experiment they showed that chromatic stimuli that cannot be distinguished on the basis of the magnitudes of the responses of the red–green and blue–yellow detection mechanisms (for example, a "purple" spot and

an "orange" spot that are theoretically metameric at the level of these detection mechanisms) are perfectly discriminable at their stimulus detection thresholds. This again suggests the existence of higher-order discriminators capable of comparing responses across the postreceptoral mechanisms. Using a noise-masking technique, Gegenfurtner and Kiper[3] argued in favor of narrowly tuned chromatic discriminators distributed about the isoluminant plane (see also Ref. 4). D'Zmura and Knoblauch[5] employed another noise-masking technique (sectored-noise masking) to demonstrate in similar fashion the presence of multiple chromatic discriminators.

The composition of these suprathreshold discriminators remains unclear. Earlier models of these discriminators focused on line-element models (see Ref. 6 for a review). These models stipulate that two chromatic stimuli are just discriminable when their respective representations in some three-dimensional space are separated by some criterion distance function. An early and well-known example of this is the set of MacAdam[7] ellipses for discriminability measured in CIE coordinates. A more recent study[8] tested a simple line-element model (a color-increment model) that required that chromatic discrimination thresholds be invariable with the suprathreshold pedestal. These results showed that the color-increment model is valid for isoluminant stimuli but fails in the presence of any luminance increment component. This result implied that there is a quantitative difference between isoluminant and luminance suprathreshold discrimination.

Furthermore, Krauskopf and Gegenfurtner[9] showed, using a pedestal paradigm, that this quantitative difference may occur between individual quadrants within the isoluminant plane (see Subsection 3.A). Hence it is still unclear whether the higher-order discriminators observed in other tasks, such as adaptation or masking, are responsible for simple chromatic discrimination between two suprathreshold stimuli throughout color space.

In our study we investigate the inputs of the red–green, blue–yellow, and luminance postreceptoral mechanisms responsible for detection to the higher-order chromatic discriminators. We use three experimental procedures. In the first we measure chromatic discrimination contours using pedestal contrasts approximately twice as great in magnitude as those used by Krauskopf and Gegenfurtner.[9] Our results provide evidence for multiple higher-order discriminators in all four quadrants of the isoluminant plane. In our second experiment we fix the test stimulus (termed a hue increment) in the direction orthogonal in our cardinal space to that of the fixed pedestal and measure the test threshold as a function of the suprathreshold pedestal contrast. We find that the test threshold varies proportionally with the pedestal contrast, suggesting that hue-increment detection is determined by the ratios of the responses of the postreceptoral mechanisms. In our third experiment we extend our findings by measuring hue-increment identification thresholds. In this procedure the hue-increment threshold was measured such that the subject could identify which of two stimuli contained a given hue increment on the basis of a recognizable color difference (e.g., to identify the bluer of two stimuli). We find that the hue-increment identification thresholds vary proportionally with the pedestal contrast. The mechanisms subserving hue-increment detection may thus play a direct role in the perception of color differences.

2. METHODS

A. Apparatus

The stimuli were presented on a Barco Calibrator CCID7651 RGB monitor driven by a Cambridge Research Systems VSG2/1 video controller interfaced with a Gateway 2000 (PC Pentium) computer. The emission spectra of the monitor phosphors were measured with a Photo Research PR-700-PC SpectraScan radiometer at the National Research Council laboratories in Ottawa, Canada. The monitor was set to a line rate of 60 kHz and a frame rate of 75 Hz, with a pixel resolution of 672×750. The screen had a mean luminance of 55 cd m^{-2} near the equal-energy white point [CIE (0.28, 0.30)]. It was viewed at a distance of 1.5 m, subtending a visual angle of 11 deg $\times$ 11 deg. The monitor phosphors were driven by a 14-bit digital-to-analog converter fed by 12- to 14-bit look-up tables. Each phosphor output was linearized by a gamma correction calculated from measurements made with a United Detector Technology (UDT S370) fitted with a radiometric detector (Model 260). A second calibration of the linearized outputs permitted a software correction that reduced the contrast error of each phosphor to within 0.017 log unit.

B. Stimuli

In all experiments the stimuli were spatiotemporally Gaussian-enveloped blobs. The use of unipolar stimuli permitted the investigation of each pole of each cardinal axis individually. The chromatic profile of these blobs was of the form

$$\mathbf{L}(x, y, t) = \mathbf{C} \exp\{-[(x/s_x)^2 + (y/s_y)^2 + (t/s_t)^2]\},$$

where $\mathbf{L}(x, y, t)$ is the cardinal color-space value at time t of the pixel whose coordinates are (x, y) relative to the center of the display, $\mathbf{C}$ is the given cardinal coordinates of the stimulus peak, and the spatial and temporal $1/e$ half-width stimulus parameters $s_{x,y,z}$ are fixed at $s_x = s_y = 0.5°$ and $s_t = 125$ ms, respectively. In all cases the stimuli were presented in a 500-ms interval preceded by a tone and were separated by 250-ms pauses.

All our stimuli are represented in a cardinal space similar to that used by Derrington et al.[10] The axes of this space were chosen to stimulate each of the three postreceptoral mechanisms individually. Using cross-axis noise masking, we have shown in previous studies[4,11] that our cardinal directions do indeed isolate these mechanisms for the two subjects concerned. Our cardinal axes were defined with previously obtained estimates of the cone-input weights to the red–green, blue–yellow, and luminance postreceptoral mechanisms.[12] In this study the cone-input weights were found to be approximately L $-$ M (red–green), S $-$ (L + M)/2 (blue–yellow), and αL + M (luminance). By use of the linear model of cone summation (see Ref. 1 for a review), each cardinal direction was computed as the unique direction that was orthogonal in cone contrast space to the color-space direction of the other two detection mechanisms. Thus, for instance, the blue–yellow cardinal direction was the cone-contrast-space (L, M, S) direction orthogonal to that of the red–green $(1, -1, 0)$ and the luminance $(\alpha, 1, 0)$ mechanisms given directly by their respective cone-input weights. To account for the subject-dependent parameter α,[13] a small correction ($<5°$ in cone contrast space between subjects) was made to the red–green cardinal direction on the basis of measurements of the red–green isoluminant point from a minimum-motion paradigm.[14] In a previous study[11] we showed that this correction is important when a cardinal space is used quantitatively. Apart from this correction, our cardinal directions agree with those of Derrington et al.[10]

With the discrimination procedure (described below), all three cardinal axes were scaled by use of a measurement of the detection threshold along each cardinal axis. As opposed to a Cartesian (rg, by, lum) cardinal representation, we used a spherical system that defined three stimulus quantities—contrast C, azimuth θ, and elevation ϕ—such that

$$C = \sqrt{(rg^2 + by^2 + lum^2)},$$

$$\theta = \sin^{-1}[by/\sqrt{(rg^2 + by^2)}],$$

$$\phi = \sin^{-1}[lum/\sqrt{(rg^2 + by^2 + lum^2)}]. \tag{1}$$

The contrast of the stimulus thus denotes the distance in cardinal space between the stimulus and the origin (neutral white) and therefore corresponds, crudely, to the

stimulus saturation.   In our cardinal space we shall use cardinal units as the quoted unit of contrast.   The azimuth represents the direction of the isoluminant component of the stimulus and therefore relates to the perceived hue.   The elevation indicates the relative magnitude of the achromatic component.

C. Subjects
The two authors participated as subjects in these experiments.   Both were color normal as tested by the Farnsworth–Munsell 100-hue color test and wore their usual optical corrections.

D. Experimental Paradigms

1. Fixed-Pedestal Discrimination
In this paradigm a discrimination procedure was used. The pedestal stimulus was fixed at a given contrast in each of the four quadrants [Fig. 1(a)].   This pedestal contrast was fixed at 15 and 12.5 units in cardinal space for subjects MJS and KTM, respectively.   The discrimination threshold was measured in 12–16 test directions in the isoluminant plane.   The discrimination contour thus mapped was compared with a detection contour that was obtained over the same range of test directions but with no pedestal.   The aim of this experiment was therefore to determine the effect of the presence of each pedestal on the ability to discriminate tests sampled throughout the isoluminant plane.

2. Hue-Increment Detection
The discrimination procedure was also used in this paradigm.   The pedestal was fixed at one of six or seven contrasts in one of at least 16 directions in the isoluminant plane [Fig. 1(b)].   The test was fixed in a direction orthogonal (counterclockwise) in cardinal space to the pedestal.   Because the addition of the test approximated a change in the stimulus azimuth in cardinal space, the test in this paradigm will be referred to as a hue increment. For each pedestal direction the test discrimination threshold was plotted as a function of pedestal contrast. This paradigm permitted us to compare hypothetical models of the suprathreshold discriminators.

3. Hue-Increment Identification
In the third paradigm an identification procedure was used.   The pedestal was fixed at a given contrast in one direction in each of the four quadrants in the isoluminant plane [see Fig. 1(c)].   In contrast to the hue-increment detection paradigm, the test consisted of both a component orthogonal in cardinal space to the pedestal color-space direction (a hue increment) and a component parallel to the pedestal color-space direction (a contrast increment). For each pedestal, 25 test conditions were used, consisting of cross sampling between five contrast-increment values and five hue-increment values.   The hue-increment threshold was measured, that is, the magnitude at which the subject could identify the test stimulus on the basis of a perceived color difference (e.g., more blue) relative to the pedestal alone.   As with the hue-increment detection paradigm, this paradigm was used to investigate the link between the postreceptoral detection mechanisms and the
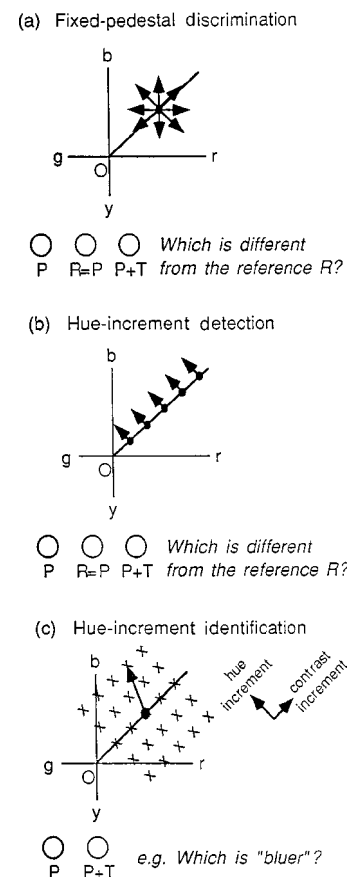

Fig. 1.   Experimental paradigms.   In each experiment a pedestal, P (solid circles), and a pedestal + test, P + T (arrow heads), were presented in random order.   In (a) and (b) the subject was presented a temporal sequence of three stimuli: The pedestal was presented twice and the pedestal + test once.   The middle stimulus (the reference) was always the pedestal only.   The subject was required to report which of the other two stimuli (the first or the third) was different from the reference.   In (c) the subject was required to make a color comparison, e.g., which stimulus was the bluer of the two stimuli presented.   Axes represent the two isoluminant cardinal axes red–green (r–g) and blue–yellow (b–y).

suprathreshold chromatic discriminators and furthermore to determine whether the chromatic discriminators contribute directly to the perception of color differences.

E. Threshold Measurement Procedures

1. Discrimination Procedure
Discrimination thresholds were measured with a two-alternative forced-choice staircase procedure modified to resemble a three-stimulus, two-choice oddity task.   In each trial three stimuli were presented in temporal sequence: a pedestal-only stimulus occurred twice and a pedestal + test stimulus once.   The middle presentation was always a pedestal-only stimulus, and the subject was required to choose whether the first or the third presentation contained the test stimulus (the "odd one out"). The pedestal was fixed in color space.   The test stimulus was fixed in a direction orthogonal to the pedestal, but its magnitude was varied.   The object of the experiment was to determine the test stimulus magnitude at which the pedestal and pedestal + test could be reliably discriminated.

A standard staircase procedure was used, and audio feedback was provided. In each measurement the detection threshold of the test stimulus was determined by the last six reversals of an eight-reversal staircase. The staircase step-size (-0.05 log unit after two consecutive correct responses, $+0.1$ log unit after an incorrect response) converged at the 81.6% correct level. An average of at least three measurements was used to determine the threshold value.

2. Identification Procedure

Identification thresholds were measured with the method of constant stimuli. Each presentation consisted of two stimuli: the pedestal and the pedestal + test, displayed in random order. The pedestal was fixed in color space in each threshold measurement. Following each two-stimulus presentation, the subject was required to signal which stimulus contained specified color difference (redder, bluer, greener, or yellower). Since we were measuring the subject's ability to identify the hue increment, audio feedback was provided in this procedure also. Sixty presentations were used for each pedestal and test condition, and a percent-correct response was measured for each condition. The range of the hue increments was chosen so that the responses varied at least between 10% and 90%. The variation of percent response with hue increment was fitted with a cumulative Gaussian function. The fit yielded two fit parameters: a bias, which estimated the hue-increment value yielding a 50% response (veridically 0), and the hue-increment identification threshold, which estimated the hue increment, corrected for bias, giving a 81.6% response.

3. RESULTS

A. Fixed-Pedestal Discrimination

In this experiment the discrimination contours were measured with four pedestals, one in each of the four quadrants (red–blue, green–blue, green–yellow, and red–yellow) of the isoluminant plane. Each contour was determined by measuring test discrimination thresholds in 12 or 16 directions distributed throughout the isoluminant plane. These contours were compared to test detection thresholds, which were measured with an identical procedure but with no pedestal.

The results for the two subjects are shown in Fig. 2. The open triangles encircling the origin represent the test detection thresholds with no pedestal. The solid circles are the discrimination threshold contours for each pedestal condition. For clarity, both the detection and the discrimination thresholds have been scaled by a factor of 3. The open triangles represent the test detection data translated by the pedestal vector. This permits a direct comparison between the detection and the discrimination contours for each pedestal condition. In this way we are able to show how the presence of each pedestal affects the discrimination of the test over the gamut of test directions.

Following a similar procedure but using lower pedestal contrasts, Krauskopf and Gegenfurtner[9] showed that the effect of the pedestal depended on the pedestal direction. They observed that for pedestals in the green–blue (top

left in Fig. 2) and red–yellow (bottom right) quadrants there was a selective elongation of discrimination thresholds relative to detection thresholds along the pedestal direction. They observed, however, that for pedestals in the red–blue (upper right) and green–yellow (lower left), quadrants, there was no selective elongation of the discrimination contour relative to that for detection. By approximately doubling the pedestal contrast from those used by Krauskopf and Gegenfurtner, we confirm the presence of selective elongation along the pedestal direction for green–blue and red–yellow pedestals but furthermore demonstrate the occurrence of elongation in the other two quadrants. Such elongation is particularly pronounced for subject MJS but is also evident for subject KTM. Elongation of the contours along the direction of each added pedestal indicates the presence of suprathreshold discriminators tuned specifically to each pedestal color-space direction.[9] Our finding therefore argues for the presence of suprathreshold discriminators that are distributed throughout the isoluminant plane. In the re-
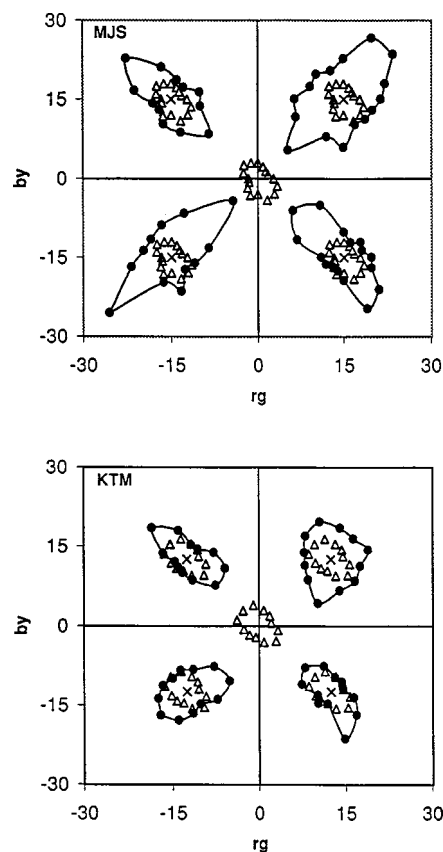

Fig. 2. Fixed-pedestal discrimination contours in the isoluminant plane for two subjects. The axes represent the red–green (rg) and blue–yellow (by) cardinal directions. The open triangles encircling the origin represent the detection threshold measurements (no pedestal). The solid circles in each quadrant represent the discrimination thresholds relative to the fixed pedestal (crosses). For clarity both the detection and the discrimination measurements have been scaled by a factor of 3. The open triangles enclosed in each discrimination contour represent the translation of the detection measurements from the origin to the fixed pedestal. The results for both subjects show that discrimination contours are elongated in the pedestal direction relative to the detection contours, suggesting the presence of multiple distributed suprathreshold discriminators.
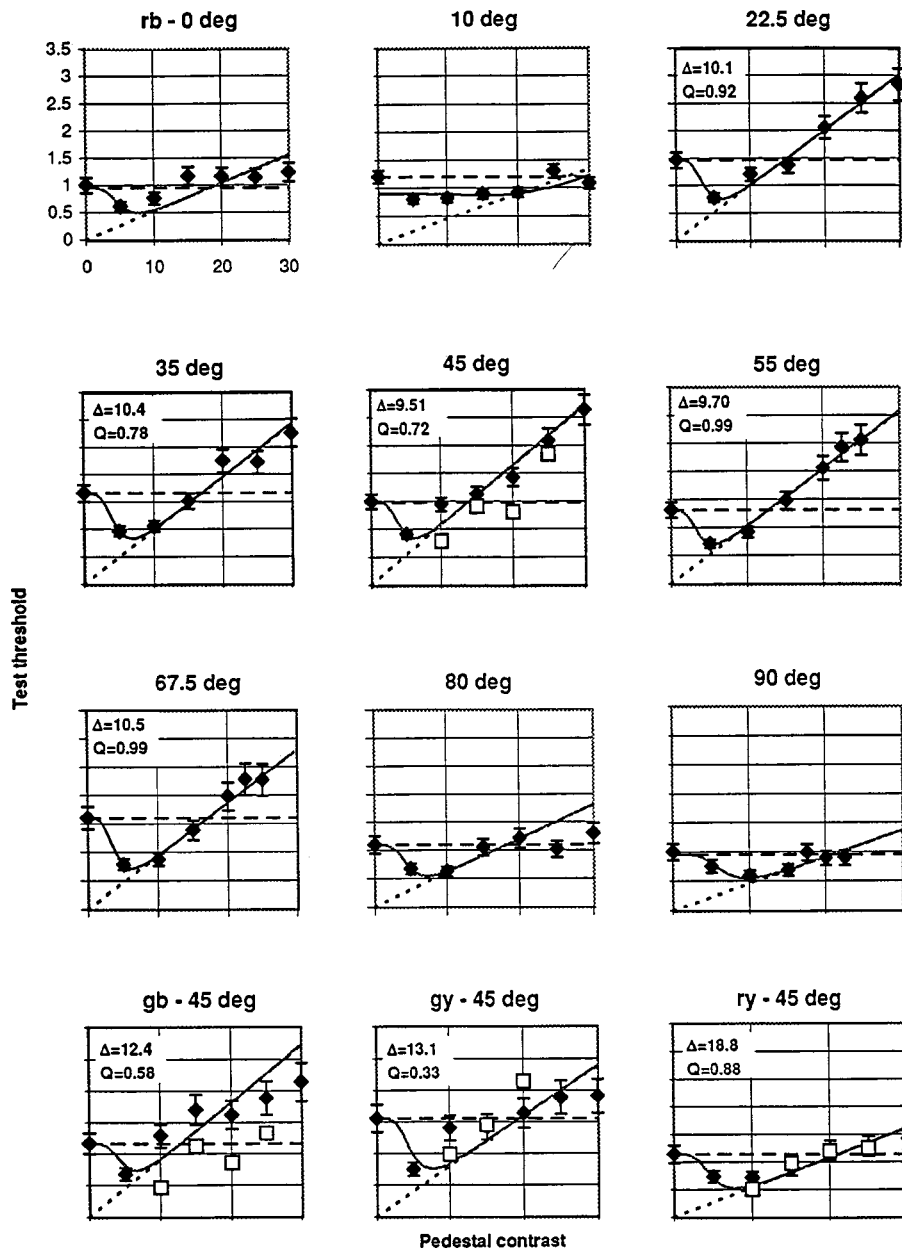
Fig. 3.   Hue-increment detection thresholds for subject MJS.   The figure shows thresholds for nine pedestal directions in the red–blue (*rb*) quadrant of the isoluminant plane (top three rows) and for one (45-deg) direction in each of the green–blue (*gb*), green–yellow (*gy*), and red–yellow (*ry*) quadrants (bottom row).   The horizontal axis represents the pedestal contrast, and the vertical axis represents the test threshold.   The test was orthogonal to the pedestal in cardinal space.   Horizontal dashed lines represent the prediction that the test threshold will be constant, and sloping dotted curves represent a proportional representation between test threshold and pedestal contrast.   Solid curves portray a composite model: constant test thresholds at low pedestal contrasts and proportional test thresholds at high pedestal contrasts.   The D value represents the inverse of the fitted slope of a linear regression, and Q represents the goodness of the regression fit ($0 < Q < 1$), a Q value exceeding 0.1 taken to be a good fit.   Open squares represent measurements of test thresholds under conditions of pedestal-contrast jitter (see Section 4).

maining experiments we investigate the inputs to these discriminators.

B.   Hue-Increment Detection
In this experiment we tested the effect of changing pedestal contrast on hue-increment detection.   The direction of the test was fixed so as to be orthogonal in cardinal space to that of the pedestal.   The superposition of this test corresponds to the addition of a hue increment while the contrast is kept fixed.   This experiment investigates how sensitivity to hue increments varies for different pedestal contrasts.   We specifically compared two predictions of this dependence.   The first prediction is that the test discrimination threshold will remain invariant with pedestal contrast, which argues for a color-increment hypothesis based on a simple line-element model.[8]   The second prediction is that the test discrimination will vary proportionally with the pedestal contrast, which argues for the presence of discriminators that are dependent on the ratio of the postreceptoral detection mechanism outputs.   For this reason, we refer to the latter hypothesis as a ratio model.
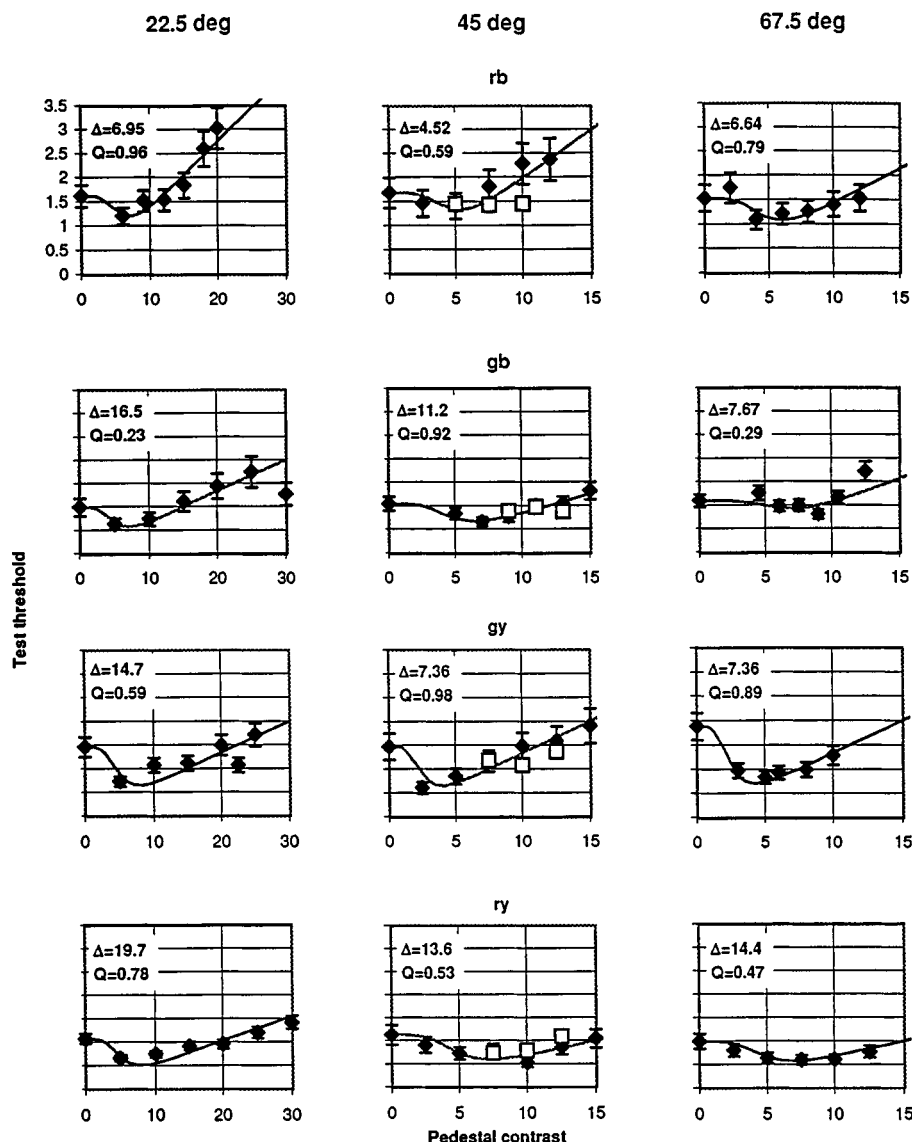
Fig. 4.   Hue-increment detection thresholds for subject KTM in intermediate directions of the isoluminant plane.   The figure shows thresholds measured with pedestals fixed in three directions in each of the four quadrants (*rb, gb, gy, ry*) of the isoluminant plane. Symbols and results are the same as in Fig. 3.

Test discrimination threshold is plotted against pedestal contrast for subjects MJS (Fig. 3) and KTM (Figs. 4 and 5).   The top three rows of Fig. 3 show the hue-increment thresholds in nine pedestal directions in the red–blue quadrant of the isoluminant plane, beginning with the 0 deg pedestal (red cardinal axis) in the top-left panel and ending with the 90 deg pedestal (blue cardinal axis) in the bottom-right panel.   The bottom row of Fig. 3 shows discrimination thresholds for oblique (45 deg) pedestal directions in the other three quadrants.   The horizontal, dashed line in each plot of Fig. 3 represents the prediction that the test discrimination threshold will be constant and equal to the detection threshold of the test stimulus alone.   This prediction, based on a line-element model, clearly cannot explain two features of the data— the reduction of hue-increment threshold at relatively low pedestal contrasts and the elevation of hue-increment threshold at high pedestal contrast.   The sloping dotted curve in Fig. 3 represents the prediction that the test dis-

crimination threshold will vary proportionally (by some fitted-slope constant λ) with pedestal contrast.   For pedestal contrasts above some transition contrast π, this model is clearly more satisfactory than the line-element model.   Our results therefore support a ratio model of suprathreshold hue-increment detection above a particular pedestal contrast.

The ratio model does not, however, satisfactorily explain hue-increment thresholds at low pedestal contrasts. There is a transition from test-alone detection at sub- and near-threshold pedestal contrasts to hue-increment detection at suprathreshold pedestal contrasts as described by the ratio model.   To incorporate this transition, the ratio model (solid curve) fitted to the data of Figs. 3–5 was of the form

$$T = k_1(T_0) + (1 - k_1)(P/\Delta). \qquad (2)$$

T is the test threshold at a pedestal contrast P and T_0 is the test detection threshold in the absence of a pedestal.

$k_1 = \pi^4/(\pi^4 + P^4)$ is an arbitrary switching parameter enabling the transition between low and high pedestal contrasts: π is the pedestal contrast (the transition contrast) at which the low- and high-pedestal-contrast be-
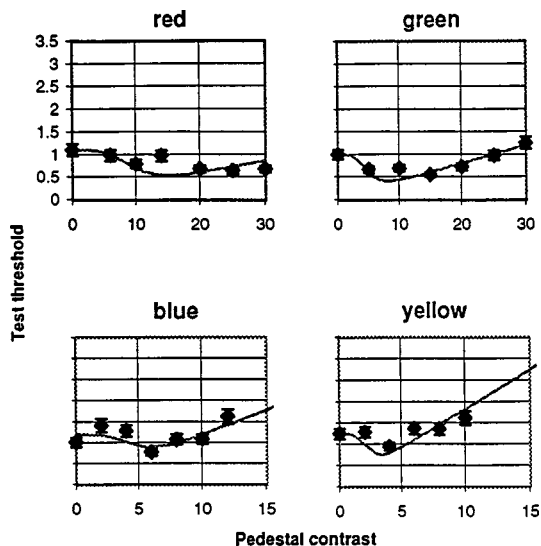

Fig. 5. Hue-increment detection thresholds for subject KTM in cardinal directions of the isoluminant plane. The figure shows thresholds measured with pedestals fixed along each of the four cardinal axes (red, blue, green, yellow). Symbols as in Fig. 3.

haviors have equal weighting. $\Delta = 1/\lambda$ represents the inverse of the slope of the linear portion of the variation and will be referred to as the hue discriminability: The greater the discriminability, the better the resolution between two neighboring stimuli. The fitted parameters were the transition pedestal contrast π and the discriminability Δ for each pedestal color-space direction.

These fitted values of the discriminability parameter Δ are plotted in Fig. 6. In three of the four panels the data for two different quadrants have been overlain. The pedestal directions 0 and 90 deg refer in all cases to cardinal directions. Color-space directions removed from these axes will be referred to as intermediate directions. These plots show that the discriminability is constant for intermediate directions (between 15 and 75 deg) in each quadrant. However, discriminability varies considerably for pedestal directions (and, therefore, test directions) near the cardinal axes. The fits for subject MJS in Fig. 3 suggest that this variation arises from the presence of an upper bound on the test threshold when the model would otherwise tend to exceed the test detection threshold (the flat dashed line). This finding indicates that test stimuli in the cardinal directions can be discriminated in isolation from the pedestal, independent of the pedestal contrast. We also note that the same test–pedestal relationships were observed for tests and pedestals in the
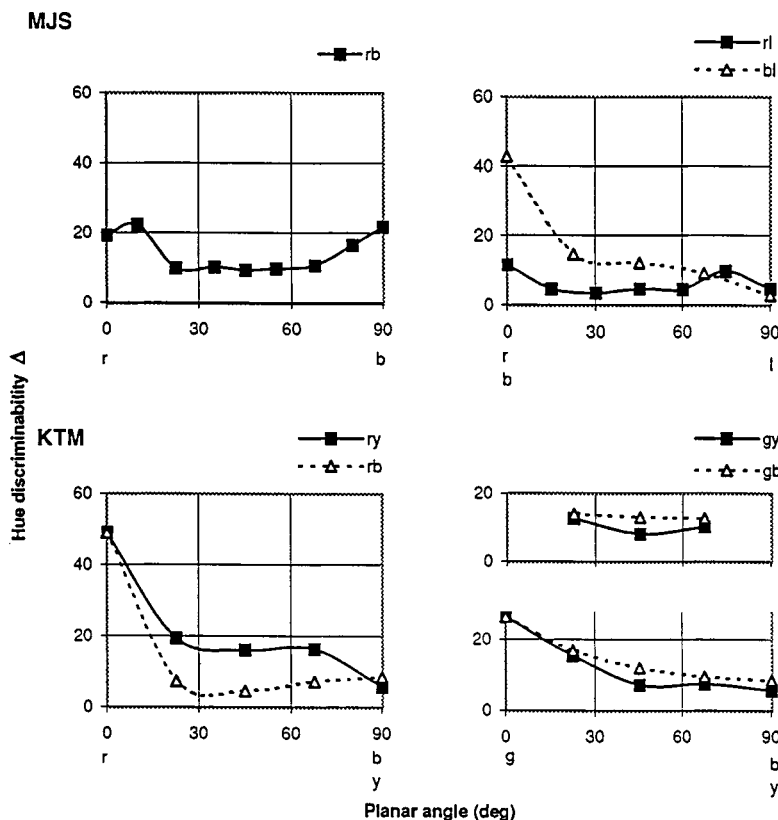

Fig. 6. Hue discriminability as a function of pedestal direction in color space. The figure shows results for pedestals in the red–blue (top left), red–luminance, and blue–luminance (top right) quadrants for MJS and for pedestals in the red–blue and red–yellow (lower left) and green–blue and green–yellow (lower half of lower-right panel) quadrants for KTM. Horizontal axes represent the pedestal direction, whose end points are labeled, accordingly, *r*, red; *b*, blue; *g*, green; *y*, yellow; *l*, luminance. The vertical axis represents hue discriminability, which is determined as the inverse of the fitted slope of the proportional relation between test threshold and pedestal contrast. The figure shows that discriminability is constant for pedestal directions more than 15 deg from the cardinal axes, i.e., directions between 15 and 75 deg in each quadrant. The upper overlay in the bottom-right panel represents the discriminability for this condition adjusted for a 0.15 log-unit underestimation of the green cardinal-axis unit (see Section 4).

isoluminant plane and those in the red–green/luminance and blue–yellow/luminance planes for the one subject tested (MJS). This finding suggests that there is no fundamental difference between isoluminant and nonisoluminant suprathreshold discrimination. Finally, we note that the fitted values of the transition contrast π are remarkably stable: 4.7 ± 1.2 over all intermediate pedestal directions and subjects. Thus ratio-dependent hue-increment detection occurs only when both the red–green and the blue–yellow mechanisms are stimulated at contrasts at least five times above their combined threshold.

Figure 7 shows the variation of the discriminability parameter as the pedestal is fixed in different directions in the isoluminant plane. The figure is a replot of Figs. 3–5 such that the pedestal and test axes are simultaneously rotated to illustrate the direction of the pedestal in the isoluminant plane. In this plot, therefore, the ratio model predicts that the hue-increment discrimination thresholds will form radial zones (shaded) converging at the origin. The central axis of each shaded zone represents the pedestal direction, and the asterisks plot the test thresholds (perpendicular distance from this axis) as a function of pedestal contrast (distance along the axis from the origin). The boundaries of each shaded zone represent the ratio-model fit to the threshold data (line through the data points) and its reflection about the pedestal axis. The angular half-width of each zone therefore represents the arc cotangent of the fitted discriminability parameter Δ. The figure shows that the width of each zone is constant with respect to pedestal direction, implying that hue discriminability as expressed in cardinal units is uniform throughout the isoluminant plane. The implication of this finding is that the mechanism underlying hue-increment detection not only depends on the ratio of normalized postreceptoral responses but is actually derived directly from this ratio (see Section 4).

To evaluate the ratio model quantitatively, we estimated the Q coefficient of linear regression fits to each test-pedestal function in Figs. 3 and 4 (endnote 1 of Ref. 15). The Q coefficient estimates the probability, assuming a χ^2 random-error distribution, that the regression residuals were obtained by chance and not as the result of a systematic error in the model. A Q coefficient exceeding 0.1 is taken as a good fit to the data.[16] The inverse of the fitted slope (the discriminability Δ) and the Q value for each regression are shown in each panel of Figs. 3 and 4. The Q coefficients for both subjects all exceed the goodness criterion of 0.1, and 16 out of the 20 fits yield Q coefficients exceeding 0.5. The ratio model therefore provides a good fit to our hue-increment threshold data. We further tested the hypothesis that the fitted discriminabilities Δ were uniformly distributed about the isoluminant plane for each subject. The Q coefficients for this hypothesis were 0.21 for MJS and 0.76 for KTM. Thus the hypothesis that hue discriminability is constant throughout the isoluminant plane cannot be rejected on the basis of our data.

C. Hue-Increment Identification

In this experiment we tested whether the thresholds for identifying the hue increment differed from the thresholds for detecting the hue increment. In each measure-
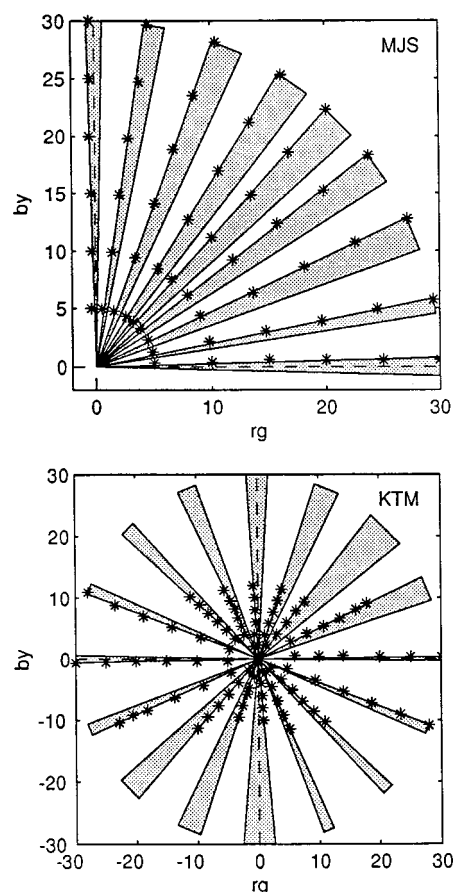

Fig. 7. Discrimination zones in the isoluminant plane for two subjects. The figure shows measurements for subject MJS with pedestals in the red–blue (*rb*) quadrant and for subject KTM with pedestals throughout the isoluminant plane. The pedestal is represented in the appropriate direction in cardinal space (the bisecting direction of each shaded area). The data points (*) represent the hue discrimination thresholds illustrated in Figs. 3–5. For clarity these thresholds have been scaled by a factor of 0.5. Each line through the data points represents the fit of a proportionality relationship between hue-increment threshold and pedestal contrast. The other (clockwise) boundary of each shaded zone is the reflection of this line about the pedestal direction. The figure shows that the angular width of the discrimination zones in cardinal space is constant throughout the isoluminant plane.

ment the pedestal was fixed at a medial contrast (12.5 or 15 contrast units) in an intermediate ($\pm 45°$) direction in cardinal space. For each pedestal/pedestal + test presentation the subject was required to determine, using an appropriate color-difference cue, which of two stimuli contained a given hue increment relative to the other. Thus, for example, with a red–blue pedestal, the subject's task was to select the bluer of two stimuli, whereas with a green–blue pedestal, the greener stimulus was to be selected. In this experiment the test vector consisted of two components: a contrast increment parallel to the pedestal vector and a hue increment orthogonal in cardinal space to the pedestal vector (Fig. 8). For each value of contrast increment, the subject response following the given criterion (as a percentage of stimuli presented) was plotted as a function of the hue increment. A cumulative Gaussian fit was used to determine the hue-increment identification threshold at each contrast-increment value.

The objective of the experiment was to determine the variation of this identification threshold with the contrast-increment value for each of the four pedestal directions.

The results for the four pedestal directions are shown in Fig. 9. The horizontal axis shows the net contrast of the pedestal + test stimulus, i.e., the pedestal contrast plus the contrast increment. The vertical axis plots the hue-increment identification threshold. The data show that, for pedestal + test contrasts exceeding a particular value (~6 contrast units), the variation can be described by a proportional relationship. The striking similarity between this characteristic for hue-increment identification and that for hue-increment detection in the previous experiment suggests that the respective underlying mechanisms are intrinsically linked. Furthermore, our results show that the ratio model accounts for hue-increment identification thresholds even when the pedestal and pedestal + test contrasts are significantly different. This implies that hue-increment identification ignores such contrast differences, suggesting an inherent separability between hue and contrast discrimination.

4. DISCUSSION

The results of our experiments are as follows. First, we provide evidence that suprathreshold chromatic discrimination within the isoluminant plane is subserved by multiple mechanisms distributed about the plane. Sec-
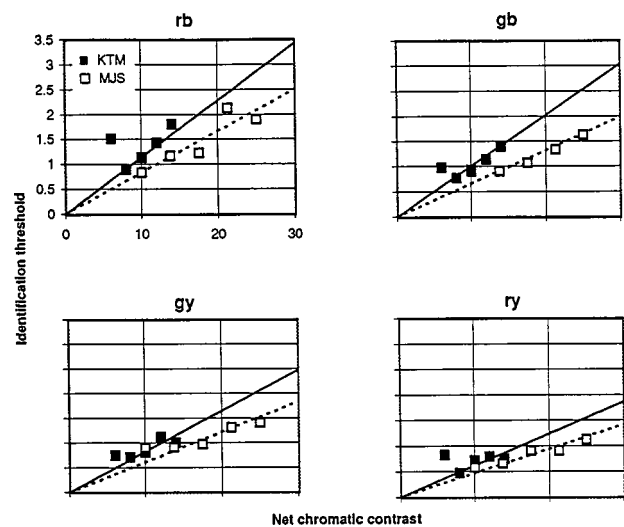

Fig. 9. Hue-increment identification threshold as a function of net chromatic contrast. The identification threshold was measured for each test chromatic contrast value with a cumulative Gaussian fit to a constant-stimulus paradigm (see Fig. 8). Net chromatic contrast is given by the sum of the pedestal contrast and the test contrast increment. The figure shows that the identification threshold varies proportionally with net chromatic contrast at high chromatic contrast values. This similarity to hue-increment detection thresholds (Figs. 3–5) suggests that the mechanisms for hue-increment detection and identification are directly linked and that the latter subserves the perception of color differences.

ond, we observe that the hue-increment detection threshold is proportional to the pedestal chromatic contrast, with the result that isoluminant discrimination is restricted to radial zones in a cardinal color space. This finding suggests that hue discrimination is based on a ratio comparison of postreceptoral detection mechanism outputs. The uniform discriminability within each quadrant suggests that the discriminator response is evaluated as the ratio of these detection mechanism responses normalized to their respective thresholds. Third, we have shown that hue-increment identification is also limited to radially emanating zones in cardinal space, suggesting that the mechanisms responsible for hue-increment detection and identification serve a direct role in color-difference perception.

The evidence from our first experiment for distributed discriminators agrees with an earlier study that used multiple techniques to investigate suprathreshold discrimination.[9] With a fixed pedestal paradigm, however, this earlier study did not reveal the presence of such discriminators for the red–blue and green–yellow quadrants of the isoluminant plane in cardinal space. When we raise the contrast of these pedestals, however, our experiments reveal suprathreshold discriminators in all four quadrants of the isoluminant plane. Our result indicates that there are no fundamental differences in discrimination among the four quadrants of this plane. One possible explanation for the results of Krauskopf and Gegenfurtner[9] arises from our hue discrimination results plotted in Fig. 6. The plot for subject KTM reveals that the hue discriminability in the red–blue and green–yellow quadrants is lower (as indicated by the wider discrimination zones) than in the other two quadrants. As a
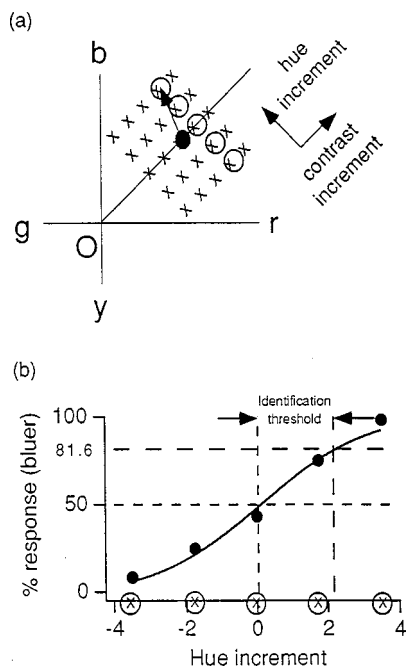

Fig. 8. Identification response as a function of hue increment. (a) The pedestal is fixed in the isoluminant plane, and the test is assigned by a constant-stimulus paradigm to one of 25 values. The test vector is resolved into two components: hue- and contrast-increment. (b) For each of the five contrast-increment values, the identification response (e.g., bluer) was tallied as a function of hue increment. For each contrast-increment value this variation was fitted by a cumulative Gaussian (solid curve), which provided a measure of the bias (50%-response test hue value) and the identification threshold (81.6%-response test hue value less the bias).

result of these differences, discrimination contours in the red–blue and green–yellow quadrants may, in general, be less elongated than contours in the other two quadrants.

Our second result demonstrates that suprathreshold discrimination is restricted to zones extending radially from the origin in cardinal space. This suggests that hue-increment detection requires some form of ratio extraction between the postreceptoral detection mechanism responses. Although few models of hue-increment detection exist, it has been suggested from other pedestal experiments that such detection is subserved by divisive inhibition of the postreceptoral mechanism outputs.[17] The quantitative form of this inhibition is as follows:

$$R_i = \frac{m_i{}^p}{\sum_j (a_{ij} m_j{}^q) + Z}, \qquad (3)$$

where R_i is the response of the ith mechanism following inhibition, m_i is the preinhibition postreceptoral mechanism response, a_{ij} is a fixed scaling factor, Z is a fixed inhibition component, and p and q are constant exponents. It is important to note that for $p \cong q$ a ratio model predicts that the postinhibition responses R_i will also be constant. Thus on the basis of our data it is impossible to distinguish between a divisive-inhibition model and a model that states that hue discriminability is determined directly by the ratio of the postreceptoral mechanism outputs (a direct-ratio model).

One difference between a divisive-inhibition model and a direct-ratio model is the predicted hue-increment detection in the presence of pedestal-contrast noise. A divisive-inhibition model predicts that such noise will increase hue-increment detection thresholds, whereas a direct-ratio model predicts that hue-increment detection thresholds will be unaffected by such noise. To test for this, we repeated our hue-increment detection measurements in the presence of a 20% pedestal-contrast jitter (Endnote 2 of Ref. 18). We observed that hue-increment thresholds did not increase, favoring a direct-ratio model (Figs. 3 and 4, open squares). We noted, in fact, that hue-increment thresholds occasionally decreased in the presence of pedestal-contrast jitter. We speculate that this threshold decrease may result from an attentional suppression of contrast-based cues and therefore from heightened attention to hue increments. The separability of hue-increment and contrast-increment detection is suggested in the identification task, in which contrast variations are present and yet hue-increment identification thresholds still obey the ratio model. This hue-versus-contrast separability indicates that these two important features of color differences (related to hue and saturation, respectively) can be distinguished at a relatively early stage of color vision. Such a distinction may play an important role in more-complex color-based processes, such as in compensation for variations in image saturation that arise from glare or shadowing.

We have argued that hue discriminability was uniform over pedestal direction in the isoluminant plane. This finding lends credence to the presence of the ratio dependence and supports the presence of a direct-ratio model,

since other models do not predict this uniformity. At the very least, this finding suggests that a threshold-normalized cardinal space is an appropriate representation, since uniformity is dependent on the choice and scaling of the color space chosen. Hence, for instance, if a cone contrast scaling were used, which scales the blue–yellow axis by a factor of 10 relative to red–green, the discrimination zones would be far narrower in pedestal directions nearer the blue–yellow axis. In a previous study,[4] we argued for the use of a cone-based space as appropriate for the analysis of cone-based mechanisms. Similarly, in this study we argue that a space based on the postreceptoral-mechanism responses is most suitable for investigating the postreceptorally based chromatic discriminators.

The effect of axis scaling on zone-width uniformity is shown in the lower-right panel of Fig. 6. In these, the hue discriminability values in the green–blue and green–yellow quadrants (KTM), there is a gradual widening of the discrimination zones toward the green axis (lower half of panel). A simple explanation for this widening lies in the fact that the scaling of the red–green axis was determined with a unipolar red cardinal stimulus. We have observed in previous studies[19] that the threshold of the green cardinal stimulus exceeds that for the red stimulus by a factor of approximately 0.15 log unit. Using this factor, we obtained corrected green–blue and green–yellow discriminability indices (top half of panel) and showed that the zone widths are now uniform. This correction illustrates the sensitivity of our discriminability measure to the chosen axes and supports the use of a threshold-normalized cardinal space in the analysis of hue-increment data.

Our results as a whole suggest that suprathreshold discrimination is performed through the extraction of the ratio of the threshold-normalized responses of the red–green and blue–yellow postreceptoral mechanisms. Such a ratio extraction is analogous to current models of velocity perception, which maintain that such perception is based on the ratio of responses of motion-detecting channels tuned to different temporal frequencies.[20,21] The presence of distributed hue discriminators provides the basis for hue-specific processes observed in other, more-complex color-related tasks. For instance, D'Zmura[22] showed that masking in color-based search paradigms is limited to masks that are close in color direction to the target. Krauskopf *et al.*[23] demonstrated, using plaid stimuli, that perceived motion is minimally coherent when the two plaid components are an orthogonal pair in any direction in the isoluminant plane of cardinal space.

Our hue-increment detection experiment produced two additional findings. First, there was a distinction between discrimination near the cardinal axes and in intermediate directions. In intermediate directions, discrimination was limited to radial zones, as explained above. In cardinal directions, discrimination could be performed, in addition, when the test component was at its detection threshold. The absence of test threshold elevation along cardinal axes agrees with a similar observation by Krauskopf and Gegenfurtner[9] in the isoluminant plane and by Cole *et al.*[24] in the red–green/luminance plane. Our results suggest that both ratio-based discriminators

and the postreceptoral detection mechanisms themselves are involved in suprathreshold discrimination. This may occur through probability summation of the responses of these different processes. Second, we observed that discrimination within the red–luminance quadrants and blue–luminance quadrants of cardinal space followed a similar pattern, with the presence of equally wide discriminability zones in intermediate directions and the intrusion by a mechanism capable of detecting the test component in isolation in cardinal directions. This argues against the presence of a distinction between luminance and isoluminant discrimination (see Ref. 8).

It is difficult from the outset to distinguish between the process of hue-increment detection away from the adaptation point and the effects of temporary changes in adaptation. The briefness ($s = 125$ ms) and smallness ($s = 0.5$ deg) of our stimuli were selected so as not to induce any alterations in the adaptation state. Our results suggest that our observed proportionality between hue discrimination threshold and pedestal chromatic contrast does not result from an adaptive process. Krauskopf and Gegenfurtner[9] observed that normalization due to adaptation is far more pronounced along the blue–yellow axis than it is along the red–green axis. This is supported by the fact that, were adaptation to be cone specific, there would be a larger effect on the blue–yellow axis than on the red–green axis. This is because the blue–yellow axis is mediated by the variation of a single cone type (the S cone), whereas the red–green axis is mediated by two opponent (L and M) cone types (see Krauskopf and Gegenfurtner[9]). Our results, on the other hand, reveal no such asymmetry between the red–green and the blue–yellow axes and show, on the contrary, that discrimination thresholds are uniformly raised with increases in red–green and blue–yellow stimulation. We therefore posit that the radial zoning of hue-increment detection is the result of the presence of chromatic discriminators and not of artifacts caused by shifts in adaptation.

Our results demonstrate that a line-element model is restricted to low-pedestal values (<5 times threshold) and to discrimination along the cardinal axes. This result may help to explain the results of a previous study.[8] In this study suprathreshold discrimination between isoluminant stimuli was found to obey a simple line-element model, whereas discrimination between two stimuli having a luminance difference falls into categorization zones that, on examination, appear to radiate from the origin. Following the conclusions of our study, it is conceivable that their isoluminant testing was performed in the low-pedestal region, in which the line-element model may be valid, whereas their luminance testing fell in the high-pedestal region, in which discrimination is limited by ratio-based hue-increment detectors. Further testing of discrimination with luminance components is necessary to test this hypothesis.

Previous studies have observed the presence of facilitation between isoluminant red–green and luminance tests and pedestals. Using grating masking, Switkes et al.[25] revealed a high degree of facilitation when the pedestal was a luminance grating and the test was red–green but showed the absence of facilitation in the reverse case. Later studies, however, revealed facilitation in both

conditions.[24,26] Mullen and Losada[26] observed that the facilitation was reduced by randomizing the superposition phase of the test and pedestal within measurements. This finding suggests that the facilitation may depend on higher-order hue-related cues. If ratio-based mechanisms such as those observed in our study mediate detection in the red–green/luminance plane, these mechanisms will certainly play a role in cross-facilitation between red–green and the luminance stimuli. This hypothesis is consistent with the data presented in the cited studies and is also consistent with the phase dependence found by Mullen and Losada.[26] Nonetheless, the presence of ratio-based mechanisms does not preclude the contribution of other factors to cross facilitation, especially in measurements that use noise masks.

The results of our third experiment suggest that the ratio-based mechanisms determining hue-increment detection play a direct role in color-difference perception. This finding therefore provides an important link between chromatic detection and hue appearance. For instance, it is now well known that the isolating stimuli for the red–green and the blue–yellow postreceptoral mechanisms do not have the appearance of unique hues.[27,28] Although the ratio-based mechanisms do not explain the appearance of unique hues, our identification task shows how they may account for comparative hues (e.g., a bluer purple). Indeed, the qualitative color differences agree with those predicted by the measurement by De Valois et al.[28] of unique-hue color-space directions; i.e., the hue increment always lay in the same hemiplane as the direction of the unique hue that best described the color difference. On the other hand, we noted that the color-difference perceptions were by no means static. With the green–blue pedestal, for instance, the "greener" stimulus appeared, on different trials, more green, less blue, or even less red. From our observations we speculate that both pedestal contrast and conditioning from previous trials may play an essential role in color-difference categorization.

The ratio-based mechanisms would clearly form part of the suprathreshold chromatic discriminators previously investigated (see Section 1). The results of our first experiment suggest the presence of narrowly tuned chromatic discriminators distributed about the isoluminant plane. From our remaining experiments it appears that continuously tuned mechanisms, each tuned to a particular ratio of postreceptoral detector responses, form the hue-increment component of suprathreshold chromatic discriminators. Our psychophysical experiments do not, however, reveal the physiological substrate of these discriminators. Krauskopf et al.[2] speculated that the chromatic discriminators are cortical in nature. Physiological data suggest that cells in the primary visual cortex encode the outputs of the red–green, blue–yellow, and luminance mechanisms in some combinatory manner, but it is uncertain what form these responses take.[29] It is possible that our hue-increment detectors do not rely on cells devoted to this purpose but instead may depend on the responses of a population of cells through probability summation[17] or dynamic coupling.[30] If, on the other hand, the ratio-based mechanisms provide the building blocks for a large number of higher-order processes, then

dedicated physiological units offer a simpler explanation of the neural architecture underlying these processes.

5. CONCLUSION

Our study provides evidence for the presence of multiple distributed mechanisms mediating suprathreshold hue discrimination in the isoluminant plane. These mechanisms derive their inputs from the ratio of the responses of the red–green and blue–yellow postreceptoral detection mechanisms. The ratio mechanisms also appear to play a direct role in the distinction of between chromatic stimuli according to perceived color differences.

REFERENCES AND NOTES

1. R. T. Eskew, Jr., J. S. McLellan, and F. Giulianini, "Chromatic detection and discrimination," in *Color Vision: From Molecular Genetics to Perception*, K. R. Gegenfurtner and L. T. Sharpe, eds. (Cambridge U. Press, Cambridge, UK, 1998).
2. J. Krauskopf, D. R. Williams, M. B. Mandler, and A. M. Brown, "Higher order color mechanisms," Vision Res. **26**, 23–32 (1986).
3. K. R. Gegenfurtner and D. C. Kiper, "Contrast detection in luminance and chromatic noise," J. Opt. Soc. Am. A **9**, 1880–1888 (1992).
4. M. J. Sankeralli and K. T. Mullen, "Postreceptoral chromatic detection mechanisms revealed by noise masking in three-dimensional cone contrast space," J. Opt. Soc. Am. A **14**, 2633–2646 (1997).
5. M. D'Zmura and K. Knoblauch, "Spectral bandwidths for the detection of color," Vision Res. **38**, 3117–3128 (1998).
6. G. Wyszecki and W. S. Stiles, *Color Science: Concepts and Methods, Quantitative Data and Formulas* (Wiley, New York, 1967).
7. D. L. MacAdam, "Visual sensitivities to color differences in daylight," J. Opt. Soc. Am. **32**, 247 (1942).
8. B. A. Wandell, "Color measurement and discrimination," J. Opt. Soc. Am. A **2**, 62–71 (1985).
9. J. Krauskopf and K. Gegenfurtner, "Color discrimination and adaptation," Vision Res. **32**, 2165–2175 (1992).
10. A. M. Derrington, J. Krauskopf, and P. Lennie, "Chromatic mechanisms in lateral geniculate nucleus of macaque," J. Physiol. (London) **357**, 241–265 (1984).
11. K. T. Mullen and M. J. Sankeralli, "Evidence for the stochastic independence of the blue–yellow, red–green and luminance detection mechanisms revealed by subthreshold summation," Vision Res. **39**, 733–743 (1999).
12. M. J. Sankeralli and K. T. Mullen, "Estimation of the L-, M-, and S-cone weights of the postreceptoral mechanisms," J. Opt. Soc. Am. A **13**, 906–915 (1996).
13. C. F. Stromeyer III, A. Chaparro, A. S. Tolias, and R. E. Kronauer, "Colour adaptation modifies the long-wave versus middle-wave cone weights and temporal phases in human luminance (but not red–green) mechanism," J. Physiol. (London) **499**, 227–254 (1997).
14. P. Cavanagh, C. W. Tyler, and O. E. Favreau, "Perceived velocity of moving chromatic gratings," J. Opt. Soc. Am. A **1**, 893–899 (1984).
15. To test the ratio model, the test-pedestal functions (Figs. 3–5) were fitted by linear regression. Each test-pedestal function consisted of a number (N) of measured hue-increment thresholds (mean μ_m, standard error se_m) expressed in log units. Regression was applied to the data for each function at or exceeding a particular pedestal contrast (5 for MJS, 4 for KTM). The fit, constrained to pass through the origin, yielded a slope estimate λ, a 95% confidence interval $[\lambda_{\min}, \lambda_{\max}]$, and a sum of the squares of the residual errors ($\Sigma\,\mathrm{SE}_r^2$). An estimate of the measurement standard error (SE_m) was obtained by evaluating the means $\langle\mu_m\rangle$ and $\langle\mathrm{se}_m\rangle$ and computing the standard error in linear units with the small error approximation $\mathrm{SE}_m = \ln 10\langle\mathrm{se}_m\rangle10^{\langle\mu_m\rangle}$. The chi-squared coefficient $\chi^2 = (\Sigma\,\mathrm{SE}_r^2/\mathrm{SE}_m^2)/(N-1)$ was used to compute a goodness-of-fit parameter $Q(0 < Q < 1)$, which was the probability that the regression residuals to each test-pedestal function arose randomly. To test the uniformity of the discriminability ($\Delta = 1/\lambda$) over the isoluminant plane, we computed the mean μ_ν and the standard deviation σ_ν over ν for the M intermediate directions (>15 deg from each cardinal axis) for each subject (8 for MJS, 12 for KTM). We used the 95% confidence interval $[\Delta_{\min} = 1/\lambda_{\max}, \Delta_{\max} = 1/\lambda_{\min}]$ to estimate the measurement error $\{\mathrm{SE}_m = \mathrm{mean}[(\Delta_{\max} - \Delta), (\Delta - \Delta_{\min})]/2\}$ in each pedestal direction and computed the mean measurement error $\langle\mathrm{SE}_m\rangle$ over all directions for each subject. Again, the chi-squared coefficient $\chi^2 = (\sigma_n^2/\langle\mathrm{SE}_m\rangle^2)$ was used to compute the goodness-of-fit parameter Q for each subject.
16. W. H. Press, S. A. Teukolsky, W. T. Vetterling, and B. P. Flannery, *Numerical Recipes in C: The Art of Scientific Computing,* 2nd ed. (Cambridge U. Press, Cambridge, UK, 1992).
17. C. C. Chen, J. M. Foley, and D. H. Brainard, "Detecting chromatic patterns on chromatic pattern pedestals," in *Proceedings: Optics and Imaging in the Information Age* (Society for Imaging Science and Technology, Springfield, Va., 1997), pp. 19–24.
18. The pedestal contrasts for the first and third stimuli of each presentation were assigned random variables uniformly distributed about the nominal pedestal-contrast value with a distribution half-width of 20% the nominal contrast value. This contrast jitter was shown to raise contrast-increment thresholds by 54% (red–blue), 15% (green–blue), 108% (green–yellow), and 56% (red–yellow) at a nominal pedestal contrast of 15 for subject MJS.
19. M. J. Sankeralli and K. T. Mullen, "Independent red, green, blue, and yellow submechanisms in the cone-opponent pathways," Invest. Ophthalmol. Visual Sci. Suppl. **39**, S3 (1998).
20. A. T. Smith and G. K. Edgar, "Antagonistic comparison of temporal frequency filter outputs as a basis for speed perception," Vision Res. **34**, 253–265 (1994).
21. A. B. Metha and K. T. Mullen, "Red–green and achromatic temporal filters: a ratio model predicts contrast-dependent speed perception," J. Opt. Soc. Am. A **14**, 984–996 (1997).
22. M. D'Zmura, "Color in visual search," Vision Res. **13**, 951–966 (1991).
23. J. Krauskopf, H.-J. Wu, and B. Farell, "Coherence, cardinal directions and higher-order mechanisms," Vision Res. **36**, 1235–1245 (1996).
24. G. R. Cole, C. F. Stromeyer III, and R. E. Kronauer, "Visual interactions with luminance and chromatic stimuli," J. Opt. Soc. Am. A **7**, 128–140 (1990).
25. E. Switkes, A. Bradley, and K. K. Devalois, "Contrast dependence and mechanisms of masking interactions among chromatic and luminance gratings," J. Opt. Soc. Am. A **5**, 1149–1162 (1988).

26. K. T. Mullen and M. A. Losada, "Evidence for separate pathways for color and luminance detection mechanisms," J. Opt. Soc. Am. A **11**, 3136–3151 (1994).

27. R. T. Eskew, Jr. and M. P. Kortick, "Unique hues in 3D color space," Invest. Ophthalmol. Visual Sci. Suppl. **38**, S454 (1997).

28. R. L. DeValois, K. K. DeValois, E. Switkes, and L. Mahon, "Hue scaling of isoluminant and cone-specific lights," Vision Res. **37**, 885–897 (1997).

29. P. Lennie and M. D'Zmura, "Mechanisms of color vision," CRC Crit. Rev. Clin. Neurobiol. **3**, 333–400 (1988).

30. V. Billock, "A chaos theory approach to some intractible problems in color vision," Invest. Ophthalmol. Visual Sci. Suppl. **38**, S254 (1997).